ISTANBUL TECHNICAL UNIVERSITY ★ INSTITUTE OF SCIENCE AND TECHNOLOGY

FIELD DRIVEN HYSTERESIS SCALING IN THE D=3 ISING SPIN GLASS: HARD SPIN MEAN FIELD THEORY

Master Thesis by

Burcu YÜCESOY

Department : Physics

Programme: Physics

Supervisor : Prof. Dr. A. Nihat BERKER

MAY 2007

ACKNOWLEDGEMENTS

First of all, I want to give special thanks to Prof. Dr. Nihat Berker for his support and assistance not only on this research but also during all the seven years he was my advisor. The physicist he sees in me is the one I am always working very hard to become, so I also want to thank him for giving me a vision for the future.

Secondly, thanks to our research group for useful discussions about life, universe and everything, and also about physics, occasionally. And additional thanks to all my friends for adding some more flavor to my life the last couple of years.

Thanks to my family for their support and understanding and for not walking away when I start to talk about spins for the thousandth time. A last thank you to a special person who now may be far away in miles but never far away in my thoughts.

INDEX

LIST OF FIGURES

SUMMARY

Hysteresis loops are obtained in the Ising spin-glass phase in d = 3, using frustration-conserving hard-spin mean-field theory. The system is driven by a time-dependent random magnetic field H_Q that is conjugate to the spin-glass order Q, yielding a field-driven first-order phase transition through the spin-glass phase. The hysteresis loop area A of the $Q - H_Q$ curve scales with respect to the sweep rate h of magnetic field as $A - A_0 \sim h^b$. In the spin-glass and random-bond ferromagnetic phases, the sweep-rate scaling exponent b changes with temperature T, but appears not to change with antiferromagnetic bond concentration p. By contrast, in the pure ferromagnetic phase, b does not depend on T and has a sharply different value than in the two other phases.

1. INTRODUCTION

1.1 Spin Glasses

Spin glasses are magnetic systems in which the interactions between the magnetic moments are "in conflict" with each other, due to some frozen-in structural disorder. Thus no conventional long-range order (of ferromagnetic or antiferromagnetic type) can be established. Nevertheless these systems exhibit a "freezing transition" to a state with a new kind of "order" in which the spins are aligned in random directions [1]. In other words, spin glasses are magnetic systems which are ordered in time, but disordered in space.

The "classical" spin glass materials are noble metals (Au, Ag, Cu, Pt) weakly diluted with transition metal ions, such as Fe or Mn. However, insulators such as $Eu_xSr_{1-x}S$, with x roughly between .1 and .5, also display spin glass behavior. In the alloy picture, the scattering of the conduction electrons at the spins leads to an indirect exchange interaction which oscillates strongly with distance R.

$$J(R) = J_0 \frac{\cos(2k_F R + \varphi_0)}{(k_F R)^3} . \tag{1.1}$$

Here, J_0 and φ_0 are constants and k_F is the Fermi wave number of the host metal. Since the distances between the spins are random, some of the interaction of the considered spin with other ones will be positive, favoring parallel alignment, some negative, favoring antiparallel alignment; thus no spin alignment can be found that is satisfactory to all exchange bonds. This effect is called "frustration".

In addition to the exchange, anisotropies may play a crucial role. But there is no universal explanation for its effects. For example anisotropies of uniaxial or unidirectional character will not lead to any macroscopic global anisotropy of the system in

the disordered state, unless one dials with uniaxial spin glasses such as $(Ti_{1-x}V_x)_2O_3$. In this case, static susceptibilities have to be distinguished according to whether the field is applied parallel or perpendicular to the easy axis. Other examples of anisotropic spin glasses are ZnMn, where the easy axis is the c axis and the system is Ising type, CdMn, an example of an XY spin glass and MgMn, which shows the characteristics of a Heisenberg spin glass.

As proven by extensive experimental work over the years, in spin glasses there is a rather sharp peak in the low-frequency dependent susceptibility which then becomes progressively rounded with increasing frequency and only rather weak frequency dependence of the peak temperature. The spectrum of relaxation times broadens far above T_f and extends to macroscopic time scales at and below T_f. At the same time, equilibrium spin glass correlations develop above freezing and lead to a dramatic increase of the static nonlinear susceptibility, and the magnetization can be brought into a scaled equation of state very similar to the behavior at ordinary magnetic phase transitions. Thus the spin glass combines some features characteristic of equilibrium phase transitions with some features characteristic of nonequilibrium systems such as ordinary glasses.

Moreover, the presence of a magnetic field usually has some drastic effects on spin glasses. While the random interactions want to freeze in the spins in random directions, a magnetic field wants to align them parallel to the field, thus there is competition between spin glass order and the Zeeman energy. Therefore, strong enough magnetic fields can destroy the spin glass state entirely. Another important effect is the irreversible behavior in the temperature region of the freezing transition and lower temperatures. After switching off the field, one finds a remanent magnetization that decays so slowly with time that a nonzero remanence is observed over macroscopic time scales. This remanent magnetization also depends on the "magnetic history" of the sample. If one cycles the field from positive to negative values and then back, instead of switching it off, one observes hysteresis phenomena as in ferromagnets. However, there exists a wide variation in the shape of the hysteresis loops, which also depend on the magnetic history of the sample.

The modern theory of spin glasses began with the work of Edwards and Anderson (EA) [3], who proposed that the essential physics of spin glasses lay not in the details of their microscopic interactions but rather in the competition between quenched ferromagnetic and antiferromagnetic interactions. It should therefore be sufficient to study the Hamiltonian

$$H_{\mathcal{J}} = -\sum_{<x,y>} J_{xy}\sigma_x\sigma_y - h\sum_x \sigma_x \,, \tag{1.2}$$

where x is a site in a d-dimensional cubic lattice, $\sigma_x = \pm 1$ is the Ising spin at site x, h is an external magnetic field, and the first sum is over nearest neighbor sites only. To keep things simple, we take $h=0$ and the spin couplings J_{xy} to be independent Gaussian random variables whose common distribution has mean zero and variance one. With these simplifications, the EA Hamiltonian in Eq. (1.2) has global spin inversion symmetry. We denote by $\mathcal{J}$ a particular realization of the couplings, corresponding physically to a specific spin glass sample. It can be seen that the Hamiltonian (1.2) exhibits "frustration"; no spin configuration can simultaneously satisfy all couplings.

Anderson [4] suggested a different formulation, namely that frustration manifests itself as free energy scaling as the square root of the surface area of a typical sample. Either way, the spin glass is characterized by both quenched disorder and frustration. Their joint presence indicates the possibility that spin glasses might possess multiple pure thermodynamic states unrelated by any simple symmetry transformation.

Within months of appearance of the EA model, an infinite-ranged version was proposed by Sherrington and Kirkpatrick (SK) [5]. For a system of N Ising spins and in zero external field, their Hamiltonian is

$$H_{\mathcal{J},N} = -\frac{1}{\sqrt{N}} \sum_{1\le i\le j\le N} J_{ij}\sigma_i\sigma_j \,, \tag{1.3}$$

where the independent, identically distributed couplings J_{ij} are again chosen from a Gaussian distribution with zero mean and variance one; the $1/\sqrt{N}$ rescaling ensures

a sensible thermodynamic limit for free energy per spin and other thermodynamic quantities.

SK showed that their model had an equilibrium phase transition at $T_C = 1$. While the static susceptibility had a cusp there, so did the specific heat. This was not necessarily surprising given that infinite-ranged models are not expected to correctly describe the behavior of low-dimensional systems at the critical point. More troubling was SK's observation that the low-temperature phase had an instability; in particular, the entropy became negative at very low temperature.

A mean field theory, employing the Onsager reaction field term, was proposed two years later by Thouless, Anderson, and Palmer [6]. Their approach indicated that there might be many low-temperature solutions, possibly corresponding to different spin glass "phases". Other important early papers include the work of de Almeida and Thouless [7], who considered the stability of the SK solution in the h-T plane, and the dynamical work of Sompolinsky and Zippelius [8-10].

What is believed today to be the correct solution for the low-temperature phase of the SK model is the Parisi solution [11]. The picture that finally arose was that of a system with a new kind of symmetry breaking, known today as "replica symmetry breaking" after the mathematical procedures used to derive it. The essential idea is that the low-temperature phase consists not of a single spin-reversed pair of states, but rather of "infinitely many pure thermodynamic states" [12], not related by any simple symmetry transformations.

Concepts that arose in the study of spin glasses have led to applications in areas as diverse as computer science [13-16], neural networks [17, 18], prebiotic evolution [19-21], protein conformational dynamics [22], protein folding [23], and a variety of others.

1.2 Hysteresis

Hysteresis is a property of systems (usually physical systems) that do not instantly follow the forces applied to them, but react slowly, or do not return completely to

their original state: that is, systems whose states depend on their immediate history. The term derives from an ancient Greek meaning 'deficiency'.

Hysteresis is well known in ferromagnetic materials. When an external magnetic field is applied to a ferromagnet, the ferromagnet absorbs some of the external field. Even when the external field is removed, the magnet will retain some field: it has become magnetized.

The relationship between magnetic field strength (H) and magnetic flux density (B) is not linear in such materials. If the relationship between the two is plotted for increasing levels of field strength, it will follow a curve up to a point where further increases in magnetic field strength will result in no further change in flux density. This condition is called magnetic saturation. If the magnetic field is now reduced linearly, the plotted relationship will follow a different curve back towards zero field strength at which point it will be offset from the original curve by an amount called the remanent flux density or remanence.

If this relationship is plotted for all strengths of applied magnetic field the result is a sort of S- shaped loop. The “thickness” of the middle bit of the S describes the amount of hysteresis, related to the coercivity of the material.

Its practical effects might be, for example, to cause a relay to be slow to release due to the remaining magnetic field continuing to attract the armature when the applied electric current to the operating coil is removed.

1.3 Ising Spin Glass (Frustrated Ising Model)

The model is defined by the Hamiltonian

$$-\beta H = \sum_{<ij>} J_{ij} s_i s_j \qquad (1.4)$$

where $s_i = \pm 1$ at each site i of a cubic lattice and $< ij >$ denotes summation over nearest-neighbor pairs. The interactions (bond strengths) J_{ij} are equal to $-J$ with

quenched probability p and $+J$ with probability $1-p$, respectively corresponding to antiferromagnetic and ferromagnetic coupling.

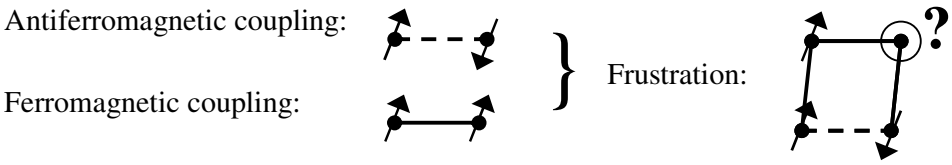

1.4 Mean Field Theory

A many-body system with interactions is generally difficult to solve exactly, except for a few simple cases. The great difficulty arises when summing over all states because of the many possible combinations of the interaction terms in the Hamiltonian. The goal of mean field theory (MFT, also known as self-consistent field theory) is to resolve these combinatorial problems.

The main idea of MFT is to replace all interactions to any one body with an average or effective interaction. This reduces any multi-body problem into an effective one-body problem. In case of the Ising Model, each spin sees the average value of its neighbors. All correlated fluctuations are ignored [24].

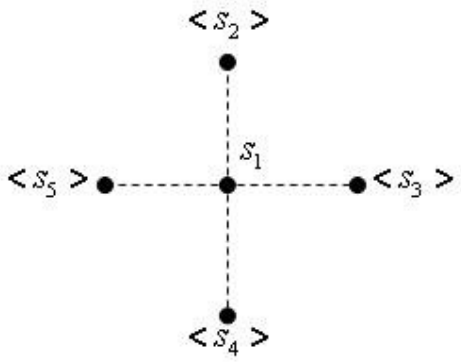

FIG. 1.1: Each spin sees the average value of its neighbors.

The self-consistent equation for the local magnetizations, $m_i =< s_i >$, is given by

$$m_i = \tanh\left(\sum_j J_{ij} m_j + H_i(t) \right), \tag{1.5}$$

where m_i can take any value between -1 and +1.

However useful the MFT is, it gives wrong results for frustrated systems. MFT uses the neighboring local magnetizations, which can take continuous values, for calculating the average at one point, thus causing the magnitudes of the conflicting interactions to be different. This artificially eliminates frustration.

1.5 Hard Spin Mean Field Theory

Hard-spin mean-field theory (HSMFT) is a method nearly as simply implemented as the conventional mean-field theory but it conserves frustration by incorporating the effect of the full magnitude of each spin. Neighboring spins themselves are used instead of their averages as in the MFT [25]. The self-consistent equation for local magnetizations m_i is

$$m_i = \sum_{\{s_j\}} \left[\prod_j P(m_j, s_j) \right] \tanh\left(\sum_j J_{ij} s_j + H_i(t) \right), \tag{1.6}$$

where the sum $\{s_{ij}\}$ is over all interacting neighbor configurations and the sum and the product over j are over all sites that are coupled to site i by interaction J_{ij}. The averages are required for the single-site probability distribution $P(m_j, s_j)$, which is $(1+m_j s_j)/2$, thus we still have a mean field approximation.

The hard-spin mean-field theory has been used in many models and calculations before [25-39]. The approach was first applied to the anti-ferromagnetic, nearest neighbor Ising model on the triangle lattice. In this case it has been known that there is no phase transition when the external magnetic field equals zero except when the temperature is also equal to zero. Conventional mean field theory in this case as well as other closed form approximations give results that are not only quantitatively incorrect but also qualitatively incorrect in that they predict a phase transition for the case of zero magnetic field for non-zero values of the temperature. This is then similar to what is predicted for an anti-ferromagnetic Ising model on a square lattice, but on the square lattice there is no frustration whereas the anti-ferromagnetic Ising

model on the triangle lattice is fully frustrated. As pointed out by Berker and Netz [25, 26], it is these frustration effects that the HSMFT correctly approximates but conventional mean field theory misses.

Besides the two-dimensional triangle lattice system HSMFT has been quantitatively successful in yielding the orderings and phase boundaries of the partially frustrated, ferromagnetically [26] or antiferromagnetically [25] stacked three-dimensional version of the model. Thus, unlike usual mean-field theory and other previous self-consistent theories, HSMFT is sensitive to qualitative differences in ordering behavior between different spatial dimensions, in fact giving exact results [27] in d=1. Immediate further applications of the method to partially and fully frustrated square and cubic lattices has yielded phase diagrams that discerned up to 24 coexisting phases and 16 magnetization sublattices, and the novel phenomena of inclusive and exclusive coexistence lines [28]. Results have also been obtained on the competition between frustration and high-spin kinematics [29]. The method is also formulated for arbitrary types of local degrees of freedom [25]

All of these systems have nearest neighbor, pair interactions. Often equally troublesome for conventional mean field theory are systems with multi-site interactions, where by multi-site we mean three or more sites. The HSMFT can be used on systems with multi-site interactions as well as pair interactions [30]. J. L. Monroe studied such systems, specifically looking at the triangle lattice Ising model system with anti-ferromagnetic pair interactions and in addition three site interactions on the elementary triangles of the lattice. His results show that as in the case for which the HSMFT was initially used, the anti-ferromagnetic Ising model on the triangle lattice, even with the addition of a three site multi-site interaction for which standard mean-field theory gives poor results the HSMFT gives topologically correct phase diagrams. In addition the quantitative values appear good when compared to Monte Carlo results for these systems.

Moreover, a free energy calculation; necessary to enable a choice when multiple solutions are found in the closed-form solution [25, 27, 31] of the theory; was presented by Kabakçıoğlu, Berker and Yalabık [32]. Consequently it is now possible within the context of HSMFT to distinguish between metastable solutions and the true thermodynamic equilibrium. Later on, A. Pelizzola and M. Pretti calculated the

zero field, zero temperature entropy and internal energy for the AF Ising model on a triangular lattice, also obtaining several informations about the model's behavior near zero temperature in their approximation [33].

Finally, a generic derivation of the HSMFT equations is presented, allowing for systematic improvements of their accuracy, which was necessary especially for the calculation of long-range correlation functions [34]. In his paper, Kabakçıoğlu also argued that the lowest level of approximation was rather inaccurate in predicting the correlation functions; nevertheless, the next level of approximation within the same framework recovered the exact result in spatial dimension d=1. At this level, HSMFT also proved to differentiate between a two-dimensional triangular and a 3D cubic lattice which was otherwise a typical failure of the mean-field theories.

2. FIELD DRIVEN HYSTERESIS SCALING IN THE D=3 ISING SPIN GLASS

Frustration and non-equilibrium effects induce complicated ordering behaviors that challenge the methods of statistical physics. Perhaps the most ubiquitous non-equilibrium effect, hysteresis is the current topic of intense fundamental and applied studies [40-44]. In the present study, hard-spin mean-field theory, developed specifically to respect frustration [26, 25], is used to study the non-equilibrium behavior of the field-driven first-order phase transition that is implicit, but to-date unstudied, in spin-glass ordering. For the Ising spin-glass on a cubic lattice, the phase diagram is obtained and the temperature- and concentration-dependent ordering of the spin-glass phase is microscopically determined. The random magnetic field that is conjugate to this microscopic order is then identified and used to induce a first-order transition and hysteresis loops. We find qualitatively and quantitatively contrasting scaling behaviors in spin-glass, quenched random-bond ferromagnetic, and pure ferromagnetic phases of the system.

The model is defined by the Hamiltonian

$$-\beta H = \sum_{<ij>} J_{ij} s_i s_j + \sum_i H_i(t) s_i \tag{2.1}$$

where $s_i = \pm 1$ at each site i of a cubic lattice and $<ij>$ denotes summation over nearest-neighbor pairs. The bond strengths J_{ij} are equal to $-J$ with quenched probability p and $+J$ with probability $1-p$, respectively corresponding to antiferromagnetic and ferromagnetic coupling. $H_i(t)$ is a linearly swept quenched random magnetic field, itself determined, as explained below, by the spin-glass local order of this system.

For our calculations we use the hard-spin mean-field theory [25-39], a method which is nearly as simply implemented as the conventional mean-field theory but which conserves frustration by incorporating the effect of the full magnitude of each spin. The self-consistent equation for local magnetizations m_i in hard-spin mean-field theory is

$$m_i = \sum_{\{s_j\}} \left[\prod_j P(m_j, s_j) \right] \tanh\left(\sum_j J_{ij} s_j + H_i(t) \right), \tag{2.2}$$

where the sum $\{s_{ij}\}$ is over all interacting neighbor configurations and the sum and the product over j are over all sites that are coupled to site i by interaction J_{ij} . The single-site probability distribution $P(m_j, s_j)$ is $(1+m_j s_j)/2$. The hard-spin mean-field theory has been used in time-dependent systems, in the study of field-cooled and zero-field cooled magnetizations in spin glasses [36].

2.1 Equilibrium Phase Diagram

The equilibrium local magnetizations $m_i^{(0)}$ are determined by simultaneously solving N coupled Eqs.(2.2) for all N sites i of the system, at zero external magnetic field, $H = 0$. For $0 < p < 1$, the system is degenerate, and many local magnetization solutions exist and are reached by hard-spin mean-field theory. The phase diagram (Fig.2.1) is obtained from temperature $T = J^{-1}$ and concentration p scans of the equilibrium spin-glass order parameter $Q^{(0)} = \frac{1}{N}\sum_i m_i^2$ and magnetization $M^{(0)} = \frac{1}{N}\sum_i m_i$, illustrated in Fig.2.2, obtained by averaging over 20 realizations for a $N = 20^3$ spin system. The results do not change if a larger system is used. In the resulting phase diagram shown in Fig.2.1, the transition temperatures are gauged by comparing T_C at $p = 0$: The precise value [45] is 4.51, the ordinary mean-field value is 6, the value obtained here is 5.06 .Thus, the transition temperatures are exaggerated as expected from a mean-field theory, but considerably improved over ordinary mean-field theory. Our obtained transition concentrations between the ferromagnetic

and spin-glass phases are $p = 0.22$, in excellent agreement with the precise value of $p = 0.23$ [46].

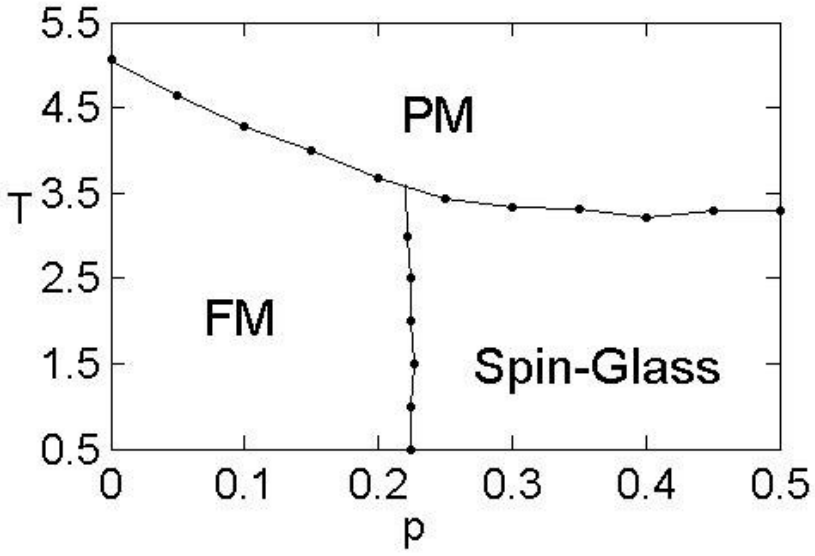

FIG. 2.1: Phase diagram from hard-spin mean-field theory for the $d = 3$ Ising spin glass. All phase boundaries are second order.

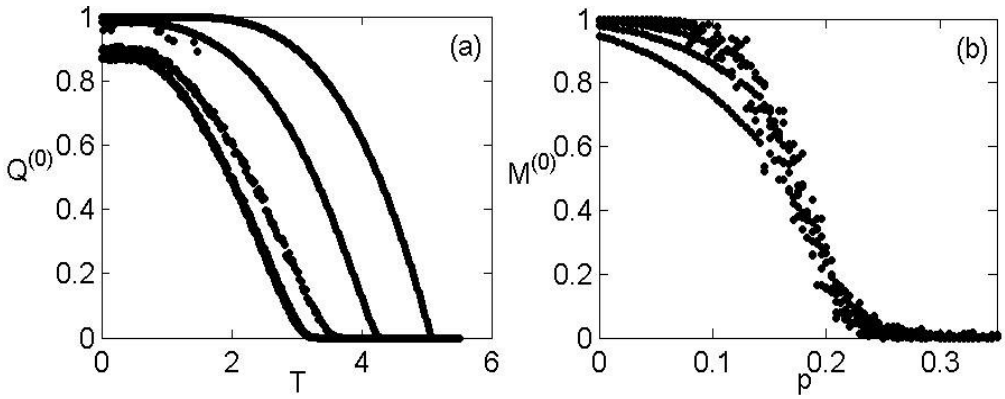

FIG. 2.2: (a) Equilibrium spin-glass order parameter $Q^{(0)}$ as a function of temperature $T = J^{-1}$. The curves, from top to bottom, are for $p =$ 0, 0.1, 0.2, 0.3, 0.5. The latter two curves overlap. (b) Equilibrium magnetization $M^{(0)}$ as a function of concentration p. The curves, from top to bottom, are for $T =$ 0.5, 1.0, 1.5, 2.0, 2.5, 3.0.

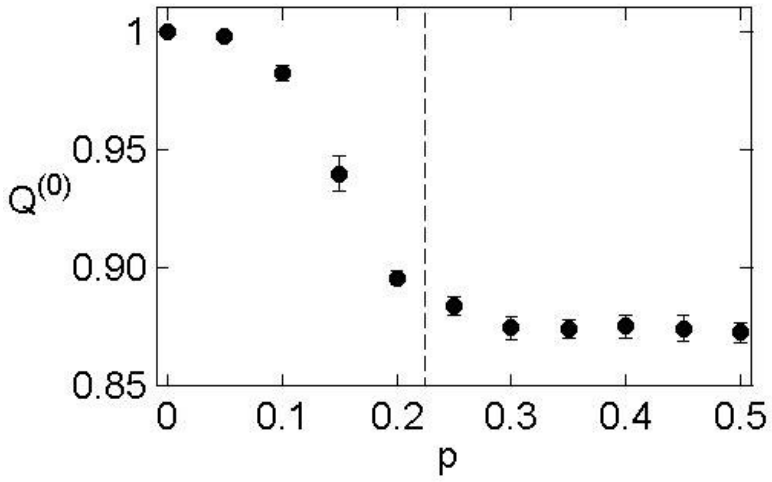

FIG. 2.3: Zero-temperature spin-glass order parameter $Q^{(0)}$ as a function of antiferromagnetic bond concentration p, obtained by averaging over 10 realizations, with the standard deviation being used as the error bar. The dashed line indicates the transition between the two phases, whose position is obtained from the phase diagram in Fig. 2.1.

Fig.2.3 shows the zero-temperature spin-glass order parameter $Q^{(0)}$ as a function of antiferromagnetic bond concentration p. It seen that, as soon as frustration is introduced via the antiferromagnetic bonds, order does not saturate at zero temperature, both in the ferromagnetic and spin-glass phases, the latter of course showing more unsaturation (Fig.2.4). Moreover, the left column of Fig.2.5 shows the equilibrium local magnetizations m_i in a cross-section of the system, in the ferromagnetic and spin-glass phases. These magnetization cross-sections are remarkably similar to the renormalization-group results [47] and are consistent with the chaotic rescaling picture of the spin-glass phase [48].

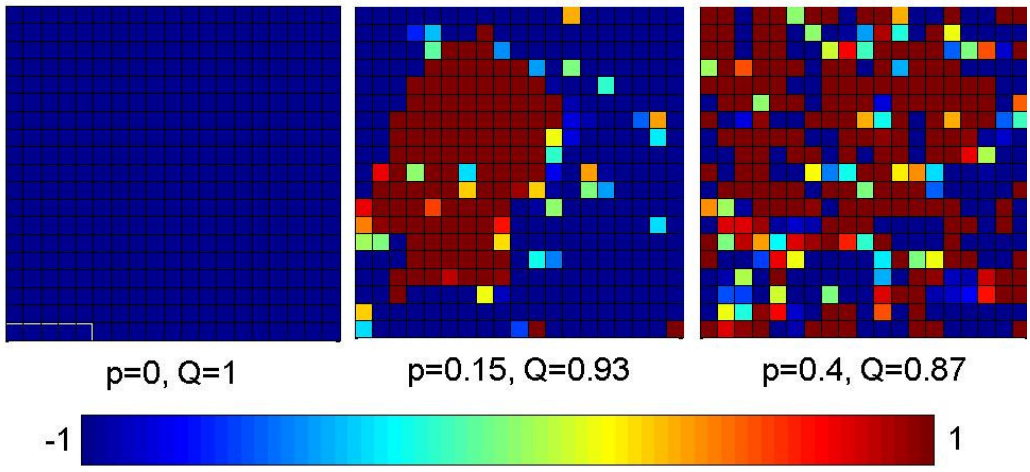

FIG. 2.4: Cross-section showing the equilibrium state local magnetizations at zero temperature. The first square shows that the pure ferromagnetic system is saturated; the magnitude of all m_i is equal to 1. The second corresponds to quenched ferromagnetic phase, where there are some m_i with $|m_i| < 1$. The last one, corresponding the spin-glass phase, shows the most unsaturation, as the number of m_i with $|m_i| < 1$ is the highest.

2.2 Spin-Glass Hysteresis Loops

The quenched random magnetic field that is conjugate to the microscopic order is $H_i(t) = H_Q(t)m_i^{(0)}$ in Eq.(2.1), where the $m_i^{(0)}$ are the equilibrium local magnetizations obtained with Eq.(2.2) for a given T, p. Hysteresis loops in the spin-glass order $Q(t) = \frac{1}{N}\sum_i m_i(t)m_i^{(0)}$ are obtained in the ordered phases, spin-glass or ferromagnetic, by cycling $H_Q(t)$ at constant T, p, via a step of magnitude h for each time unit. Thus, at time $t = 0$, $Q(t = 0) = Q^{(0)}$, the equilibrium spin-glass order parameter. A time unit is N updating of Eq.(2.2) at randomly selected sites. Thus, h is the sweep rate of the linearly driven [42-44] magnetic field. The resulting hysteresis curves are illustrated in Figs.2.6. After one cycling, the subsequent hysteresis loops for a given sweep rate coincide, and are shown in Figs.2.6 and used in the scaling analysis further below.

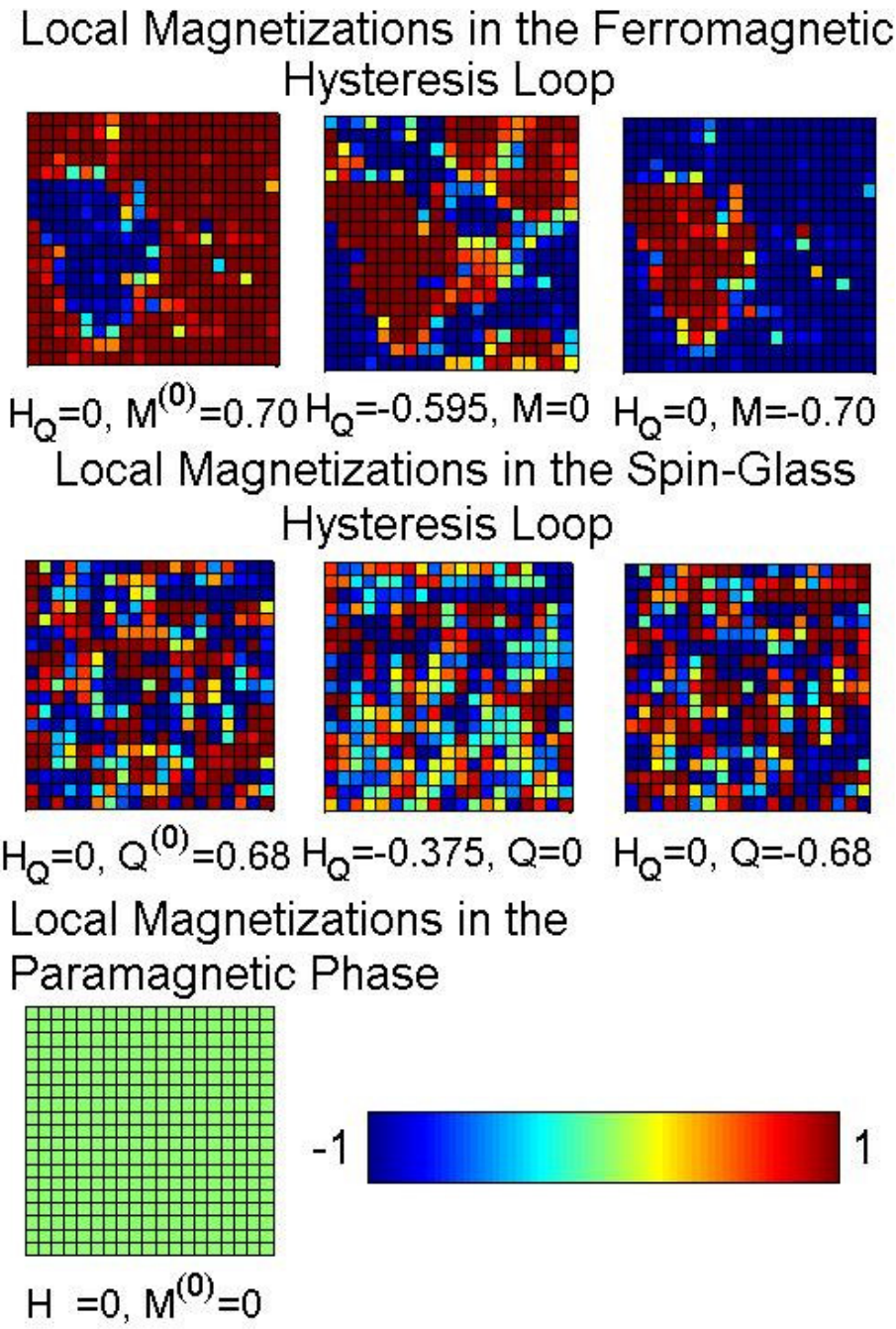

FIG. 2.5: The top-row figures are from a hysteresis loop in the ferromagnetic phase with quenched random antiferromagnetic bonds, $T = 1.5$, $p = 0.15$, $h = 0.005$. The middle-row figures are from a hysteresis loop in the spin-glass phase, $T = 1.5$, $p = 0.4$, $h = 0.005$. Left: calculated equilibrium local magnetizations $m_i^{(0)}$ in a cross-section of the three-dimensional system. A hysteresis loop is started from these systems. Middle: local magnetizations $m_i(t)$ at the first cancellation point, $M(t) = 0$ (top row) and $Q(t) = 0$ (middle row), of the first hysteresis loop. Left: local magnetizations at the first reversal point, $M(t) = -M^{(0)}$ and, $Q(t) = -Q^{(0)}$ which occurs when the first hysteresis half-loop is completed. The bottom cross-section shows the vanishing

equilibrium local magnetizations everywhere in the paramagnetic phase, to be contrasted with the spin-glass cross-section immediately above it: the global magnetization $M^{(0)} = 0$ in both cases.

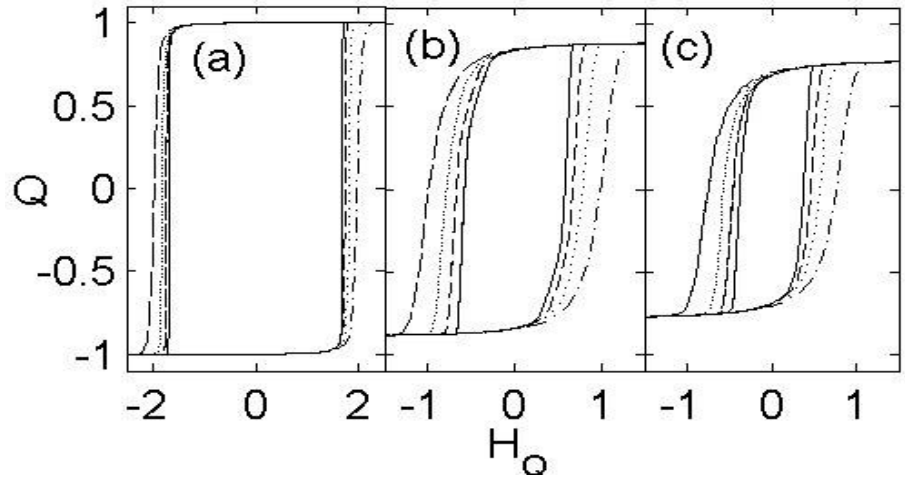

FIG. 2.6: Hysteresis loops for different values of the sweep rate h for (a) the pure ferromagnetic phase, $p = 0$, (b) the ferromagnetic phase with quenched random antiferromagnetic bonds, $p = 0.15$, (c) the spin-glass phase, $p = 0.4$, all at $T = 1.5$. The loops are, from outer to inner, for sweep rates $h = 0.05, 0.02, 0.01, 0.005$.

2.3 Cycling Effect of a Uniform Magnetic Field on Spin-Glass Order

As a contrast to the hysteretic effect of the conjugate quenched random magnetic field $H_Q(t)$ introduced above, Fig.2.7 shows the effect on the spin-glass phase of turning on and then off a uniform magnetic field $H(t)$ at a sweep rate h. As expected, the spin-glass order $Q(t)$ starts at a finite value and returns to zero, while the uniform magnetization $M(t) = \frac{1}{N}\sum_i m_i(t)$ starts at zero and returns to a finite value.

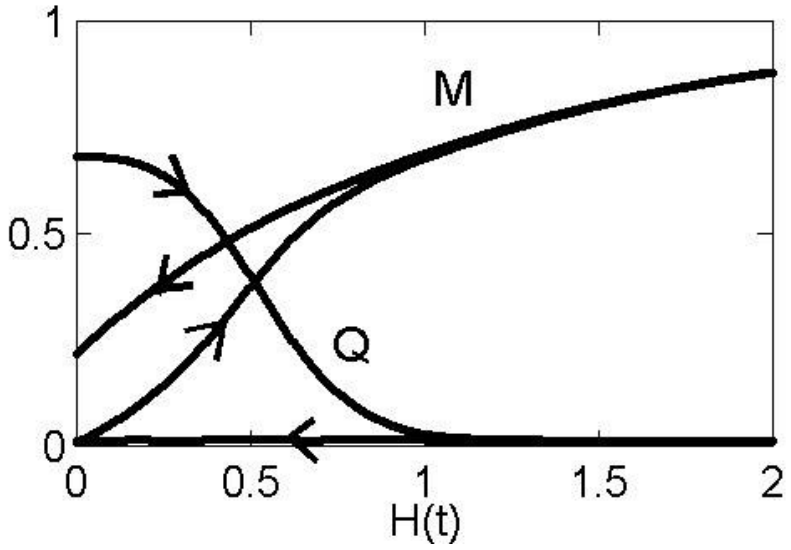

FIG. 2.7: Spin-glass order parameter $Q(t)$ and uniform magnetization $M(t)$ curves obtained when, in the spin-glass phase, the uniform magnetic field $H(t)$ is turned on and then off with sweep rate $h = 0.005$. In this figure, $p = 0.4$, $T = 1.5$.

2.4 Spin-Glass Hysteresis Area Scaling

The energy dissipation of a first-order phase transition is obtained from the hysteresis area A of the $Q - H_Q$ curve: $A = \oint Q dH_Q$. At fixed T, p, the loop area A decreases with decreasing sweep rate h and finally reaches a value of A_0. The area can be scaled as $A = A_0 + f(T)h^b$ [44]. The $(A - A_0)$ versus sweep rate h scaling curves are shown in Figs.2.8, for the pure ferromagnetic, quenched random-bond ferromagnetic, and spin-glass phases for various temperatures, where A_0 is fitted. The resulting sweep-rate exponents b are given in Fig.2.9 and Table2.1.

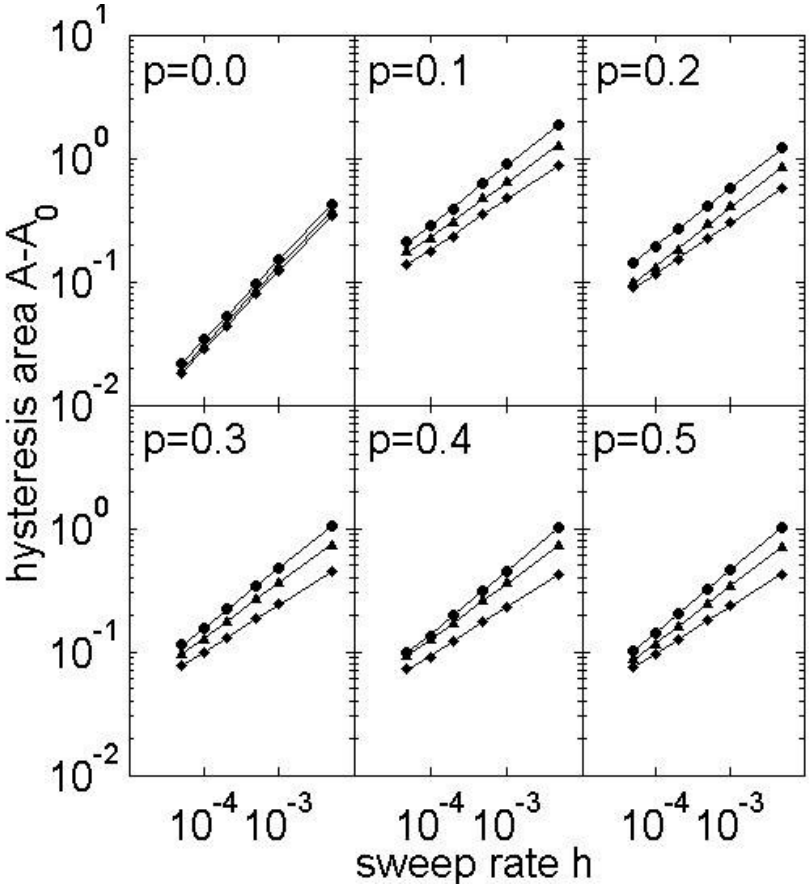

FIG. 2.8: The hysteresis area $A - A_0$ versus sweep rate h scaling curves for $T = 1.0(\bullet), 1.5(\blacktriangle), 2.0(\blacklozenge)$.

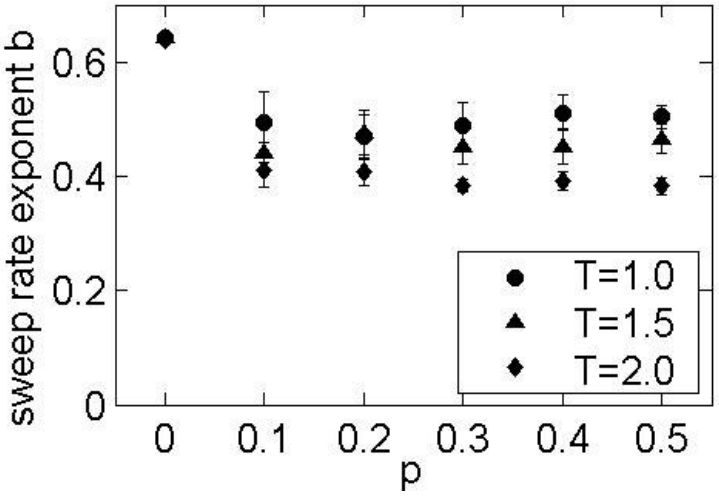

FIG. 2.9: The sweep rate exponent b versus concentration p for $T = 1.0, 1.5, 2.0$. These results are obtained by averaging over 10 realizations, with the standard deviation being used as the error bar.

TABLE 2.1: The sweep rate scaling exponents b at different temperatures and concentrations in the ferromagnetic and spin-glass phases.

T	p=0	p=0.1	p=0.2	p=0.3	p=0.4	p=0.5
1.0	0.64	0.49±0.06	0.47±0.04	0.49±0.04	0.51±0.03	0.50±0.02
1.5	0.64	0.44±0.02	0.48±0.04	0.45±0.03	0.45±0.03	0.47±0.03
2.0	0.64	0.41±0.03	0.41±0.02	0.38±0.01	0.39±0.02	0.38±0.01

3. RESULTS AND DISCUSSION

From the results given in Fig.2.9 and Table2.1, we deduce that in the pure ferromagnetic phase, $p = 0$, the exponent b is independent of temperature, as found previously [44]. However, the value of $b = 0.64$ that we find here, under hard-spin mean-field dynamics, is distinctly different from that of $b = 2/3$ found in Ref. [44] under ordinary mean-field dynamics, thereby constituting a different dynamic universality class. By contrast, in the quenched random-bond ferromagnetic phase and in the spin-glass phase, the value of b is distinctly smaller than that in the pure ferromagnetic phase, and dependent on temperature. Across both of these two phases, there appears to be no dependence of b on concentration.

In this research, we only dealt with a linearly swept magnetic field. For further investigations, the effect of a sinusoidal field can be considered. Moreover, the techniques introduced here can be used to explain many different phenomena with spin-glass-like characteristics. For example, we are considering the problem of absorbance of a polymer onto an irregular surface with randomly distributed binding points. Another interesting problem to look at would be the neural networks. These are often described as spin glass models, and hysteresis phenomena have also been mentioned in connection with them [49, 50]. Doing a more extensive research which will combine these two aspects of neural networks is also one of our future projects.

REFERENCES

[1] **K. Binder and A. P. Young,** *Rev. Mod. Phys.* **58**, 801 (1986)

[2] **D. L. Stein**, cond-mat/0301104v1.

[3] **S.F. Edwards and P.W. Anderson,** *J. Phys. F* **5**, 965 (1975).

[4] **P.W. Anderson**, *J. Less-Common Metals* **62**, 291 (1978).

[5] **D. Sherrington and S. Kirkpatrick,** *Phys. Rev. Lett.* **35**, 1792 (1975).

[6] **D.J. Thouless, P.W. Anderson, and R.G. Palmer,** *Phil. Mag.* **35**, 593 (1977).

[7] **J. R. L. de Almeida and D.J. Thouless,** *J. Phys. A* **11**, 983 (1978).

[8] **H. Sompolinsky and A. Zippelius**, *Phys. Rev. Lett.* **47**, 359 (1981).

[9] **H. Sompolinsky**, *Phys. Rev. Lett.* **47**, 935 (1981).

[10] **H. Sompolinsky and A. Zippelius**, *Phys. Rev. B* **25**, 6860 (1982).

[11] **G. Parisi,** *Phys. Rev. Lett.* **43**, 1754 (1979).

[12] **G. Parisi**, *Phys. Rev. Lett.* **50**, 1946 (1983).

[13] **S. Kirkpatrick, C.D. Gelatt, Jr., and M.P. Vecchi**, *Science* **220**, 671 (1983).

[14] **M. Mézard and G. Parisi**, *J. Phys. Lett.* **46**, L771 (1985).

[15] **Y. Fu and P. W. Anderson,** *J. Phys.* **A19**, 1605 (1986).

[16] **M. Mézard and G. Parisi,** *J. Phys.* **47**, 1285 (1986).

[17] **J. J. Hopfield**, *Proc. Natl. Acad. Sci. USA* **79**, 2554 (1982).

[18] **D. J. Amit, H. Gutfreund, and H. Sompolinsky,** *Phys. Rev. Lett.* **55**, 1530 (1985).

[19] **P. W. Anderson,** *Proc. Natl. Acad. Sci. USA* **80**, 3368 (1983).

[20] **P. W. Anderson and D.L. Stein,** 1985. Broken Symmetries, Dissipative Structures, Emergent Properties, and Life In Self-Organizing Systems, Plenum, New York.

[21] **D. S. Rokhsar, D.L. Stein, and P.W. Anderson,** *J. Mol. Evol.* **23**, 119 (1986).

[22] **D. L. Stein,** *Proc. Natl. Acad. Sci. USA* **82**, 3670 (1985).

[23] **J. D. Bryngelson and P.G. Wolynes,** *Biopolymers* **30**, 177 (1990).

[24] **H. E. Stanley**, 1971. Introduction to Phase Transitions and Critical Phenomena, Oxford University Press, New York and Oxford.

[25] **R.R. Netz and A.N. Berker**, *J. Appl. Phys.* **70**, 6074 (1991).

[26] **R.R. Netz and A.N. Berker**, *Phys. Rev. Lett.* **66**, 377 (1991).

[27] **J.R. Banavar, M. Cieplak, and A. Maritan**, *Phys. Rev. Lett.* **67**, 1807 (1991).

[28] **R.R. Netz**, *Phys. Rev. B* **46**, 1209 (1992).

[29] **R.R. Netz**, *Phys. Rev. B* **48**, 16113 (1993).

[30] **J.L. Monroe**, *Phys. Lett. A* **230**, 111 (1997).

[31] **R.R. Netz and A.N. Berker**, *Phys. Rev. Lett.* **67**, 1808 (1991).

[32] **A. Kabakçıoğlu, A.N. Berker, and M.C. Yalabık**, *Phys.Rev. E* **49**, 2680 (1994).

[33] **A. Pelizzola and M. Pretti**, *Phys. Rev. B* **60**, 10134(1999).

[34] **A. Kabakçıoğlu**, *Phys. Rev. E* **61**, 3366 (2000).

[35] **A.N. Berker, A. Kabakçıoğlu, R.R. Netz, and M.C.Yalabık**, *Turk. J. Phys.* **18**, 354 (1994).

[36] **E.A. Ames and S.R. McKay**, *J. Appl. Phys.* **76**, 6197(1994).

[37] **G.B. Akgüç and M.C. Yalabık**, *Phys. Rev. E* **51**, 2636 (1995).

[38] **J.E. Tesiero and S.R. McKay**, *J. Appl. Phys.* **79**, 6146,(1996).

[39] **H. Kaya and A.N. Berker**, *Phys. Rev. E* **62**, R1469(2000).

[40] **E. Bonnot, R. Romero, X. Illa, L. Manosa, A. Planes,and E. Vives**, cond-mat/0702211.

[41] **M.S. Pierce, C.R. Buechler, L.B. Sorensen, S.D. Kevan, E.A. Jagla, J.M. Deutsch, T. Mai, O. Narayan, J.E.Davies, K. Liu, G.T. Zimanyi, H.G. Katzgraber, O. Hellwig, E.E. Fullerton, P. Fischer, and J.B. Kortright**, *Phys. Rev. B (in press)*; cond-mat/0611542.

[42] **F. Zhong, J.X. Zhang, and G.G. Siu**, *J. Phys.: Cond. Matt.* **6**, 7785 (1994).

[43] **F. Zhong, J.X. Zhang, and L. Xiao**, *Phys. Rev. E* **52**, 1399 (1995).

[44] **G.P. Zheng and J.X. Zhang**, *J. Phys.: Cond. Matt.* **10**,1863 (1998).

[45] **A.M. Ferrenberg and D.P. Landau**, *Phys. Rev. B* **44**, 5081(1991).

[46] **Y. Ozeki and N. Ito**, *J. Phys. A* **31**, 5451 (1998).

[47] **D. Yeşilleten and A.N. Berker**, *Phys. Rev. Lett.* **78**, 1564(1997).

[48] **S.R. McKay, A.N. Berker, and S. Kirkpatrick**, *Phys. Rev.Lett.* **48**, 767 (1982).

[49] **P. Shukla and T. K. Sinha,** *Phys. Rev. E* **49**, R4811 (1994)

[50] **P. Shukla**, *Phys. Rev. E* **56**, 2265 (1997)